Atherosclerosis 370 (2023) 18–24

Contents lists available at ScienceDirect

Atherosclerosis

journal homepage: www.elsevier.com/locate/atherosclerosis

Validation and clinical impact of novel pericoronary adipose tissue measurement on ECG-gated non-contrast chest CT

Daigo Takahashi [a], Shinichiro Fujimoto [a,*], Yui O. Nozaki [a], Ayako Kudo [a], Yuko O. Kawaguchi [a], Kazuhisa Takamura [a], Makoto Hiki [a], Hideyuki Sato [a,b], Nobuo Tomizawa [c], Kanako K. Kumamaru [c], Shigeki Aoki [c], Tohru Minamino [a]

[a] Department of Cardiovascular Biology and Medicine, Juntendo University Graduate School of Medicine, Tokyo, Japan
[b] Department of Radiological Technology, Juntendo University Hospital, Tokyo, Japan
[c] Department of Radiology, Juntendo University Graduate School of Medicine, Tokyo, Japan

HIGHLIGHTS

- The CT value of non-contrast CT (NC-PCAT) is correlated with that of conventional pericoronary adipose tissue (PCAT) .
- High NC-PCAT value is associated with presence of high-risk plaque.
- NC-PCAT is a significant predictor of worse clinical outcome in coronary artery disease patients.

GRAPHICAL ABSTRACT

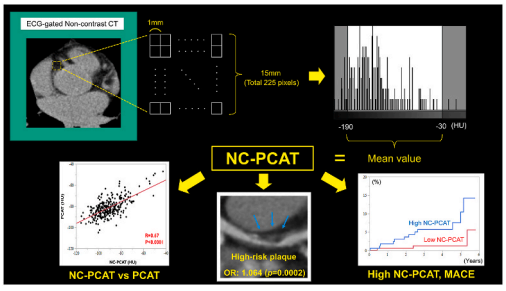

ARTICLE INFO

Keywords:
Pericoronary adipose tissue
Vascular inflammation
Computed tomography
Coronary artery disease

ABSTRACT

Background and aims: We aimed to develop a method for quantifying pericoronary adipose tissue (PCAT) on electrocardiogram (ECG)-gated non-contrast CT (NC-PCAT) and validate its efficacy and prognostic value.
Methods: We retrospectively studied two independent cohorts. PCAT was quantified conventionally. NC-PCAT was defined as the mean CT value of epicardial fat tissue adjacent to right coronary artery ostium on ECG-gated non-contrast CT. In cohort 1 (n = 300), we evaluated the correlation of two methods and the association between NC-PCAT and CT-verified high-risk plaque (HRP). We dichotomized cohort 2 (n = 333) by the median of NC-PCAT, and assessed the prognostic value of NC-PCAT for primary endpoint (all-cause death and non-fatal myocardial infarction) by Cox regression analysis. The median duration of follow-up was 2.9 years.
Results: NC-PCAT was correlated with PCAT (r = 0.68, $p < 0.0001$). In multivariable logistic regression analysis, high NC-PCAT (OR:1.06; 95%CI:1.03–1.10; $p = 0.0001$), coronary artery calcium score (CACS) (OR:1.01 per 10 CACS increase, 95%CI:1.00–1.02; $p = 0.013$), and current smoking (OR:2.58; 95%CI:1.03–6.49; $p = 0.044$) were independent predictors of HRP. Among patients with CACS>0 (n = 193), NC-PCAT (OR:1.06; 95%CI:1.03–1.10; $p = 0.0002$), current smoking (OR:3.02; 95%CI:1.17–7.82; $p = 0.027$), and male sex (OR:2.81; 95%CI:1.06–7.48; $p = 0.028$) were independent predictors of HRP, whereas CACS was not ($p = 0.15$). Multivariable Cox regression

* Corresponding author. Department of Cardiovascular Biology and Medicine, Juntendo University Graduate School of Medicine, 2-1-1 Hongo Bunkyo-ku, Tokyo, 113-8421, Japan.
E-mail address: s-fujimo@tj8.so-net.ne.jp (S. Fujimoto).

https://doi.org/10.1016/j.atherosclerosis.2023.01.021
Received 28 September 2022; Received in revised form 16 December 2022; Accepted 24 January 2023
Available online 31 January 2023

analysis revealed high NC-PCAT as an independent predictor of the primary endpoint, even after adjustment for sex and age (HR:4.3; 95%CI:1.2–15.2; $p = 0.012$).
Conclusions: There was a positive correlation between NC-PCAT and PCAT, with high NC-PCAT significantly associated with worse clinical outcome (independent of CACS) as well as presence of HRP.

1. Introduction

Coronary vascular inflammation promotes atherosclerosis and development of vulnerable plaques that result in acute coronary syndrome (ACS) [1,2]. As most of these high-risk plaques (HRPs) are non-obstructive lesions, which cannot be adequately assessed by non-invasive stress test for myocardial ischemia [3], non-invasive identification of HRP is considered challenging in clinical practice [4]. However, coronary computed tomography angiography (CCTA) can be applied to detecting characteristic features of high-risk coronary plaques such as low attenuation, positive remodeling, napkin-ring sign, and spotty calcification [5–8]. Several recent studies have reported measurement of pericoronary adipose tissue (PCAT) on CCTA as a novel method for quantifying coronary vascular inflammation, which drives the pathogenesis of ACS [9,10]. Other studies have demonstrated that PCAT is significantly associated with the presence of HRP [11,12] and that high attenuation index values of fat surrounding the right coronary artery (RCA) have a significant association with worse clinical mortality [13]. Coronary artery calcium score (CACS), measured by electrocardiogram (ECG)-gated non-contrast chest CT, is now generally recommended in screening for coronary artery disease (CAD) and risk stratification even in asymptomatic and low-risk patients [14,15]. Thus far, however, no study has reported the ability of CACS to detect vascular inflammation or HRP, which both lead to ACS. Previous studies have attempted to demonstrate the efficacy of PCAT evaluation on non-contrast CT. Some have clarified the difference between contrast CT and non-contrast CT in evaluating PCAT [16,17], and Jiang et al. has demonstrated the efficacy of radiomics to detect vulnerable plaque on ECG-gated non-contrast CT [18]. However, to the best of our knowledge, there is no established method for the accurate quantification of PCAT by non-contrast CT (NC-PCAT) or for early detection of coronary inflammation. Thus, we developed a novel method for quantification of NC-PCAT, investigated its correlation with the presence of HRP, and evaluated its prognostic value for worse clinical outcome.

2. Patients and methods

2.1. Study population and data collection

We performed retrospective analyses in two independent cohorts. The first cohort (cohort 1) was used to assess the validity of NC-PCAT and investigate the association between NC-PCAT and HRP, and included consecutive patients who had undergone clinically indicated CCTA at our institution. Fig. 1(A) shows a flow chart of the patient selection process for cohort 1. We retrospectively reviewed 504 consecutive patients with suspected CAD who had undergone both ECG-gated non-contrast CT and CCTA at our institution between August 2020 and May 2021. Those who had had cardiac surgery (n = 105) or metal implantation (i.e., coronary stents or intra-cardiac devices.) (n = 49), or had inadequate image quality (due mainly to body mass index >30 kg/m^2, n = 50) were excluded. Finally, 300 patients in total were enrolled in cohort 1. The prognostic value of NC-PCAT was determined in the

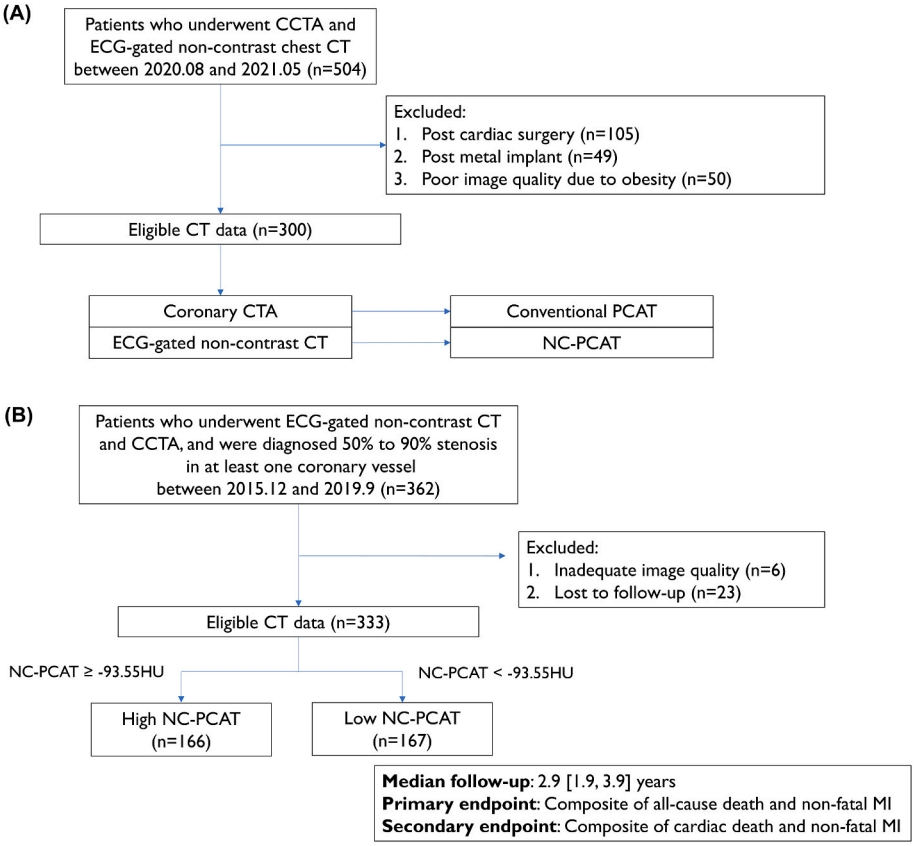

Fig. 1. Flow diagram for selection of (A) cohort 1 and (B) cohort 2.
(A) Initially, we retrospectively evaluated 504 consecutive patients who had undergone both ECG-gated non-contrast CT and CCTA between August 2020 and May 2021. Those who had had cardiac surgery or metal implantation, or whose body mass index exceed 30 kg/m^2 were excluded because of difficulty in analysis. Finally, a total of 300 patients were enrolled. (B) We retrospectively studied 362 consecutive patients, who had been diagnosed more than 50% stenotic lesions in at least one coronary artery by CCTA in our institution between December 2015 and September 2019. Those whose image quality was inadequate or were lost to follow-up were excluded, and a total of 333 patients were enrolled.

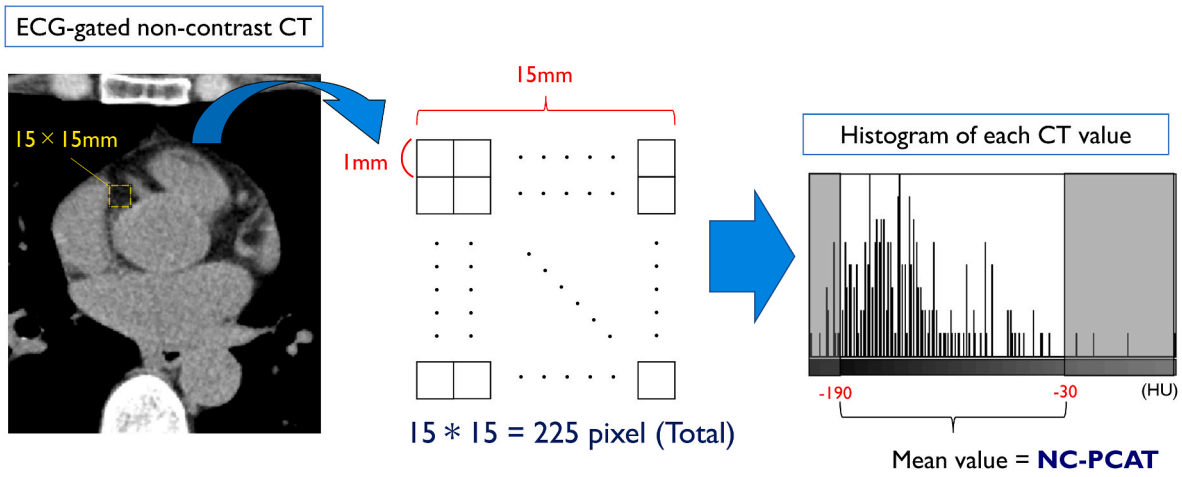

Fig. 2. Quantification of NC-PCAT.
On axial image of ECG-gated non-contrast CT, a yellow 15 × 15 mm square shows a ROI placed on pericardial fat tissue, dorsally and adjacently to the right coronary artery ostium. Mean CT values of all 225 pixels were calculated, and CT values between −190 and −30 HU were regarded as pericoronary adipose tissue. (For interpretation of the references to colour in this figure legend, the reader is referred to the Web version of this article.)

second cohort (cohort 2). Fig. 1(B) shows a flow chart of the patient selection process for cohort 2. We analyzed the data obtained in a single-center, retrospective study of 362 consecutive patients, with no prior history of CAD, who were subsequently diagnosed with a 50%–90% stenotic lesion in at least one major coronary artery by CCTA in our institution between December 2015 and September 2019. All scans were performed on a 320-detector-row CT scanner (Aquilion ONE ViSION, Canon Medical Systems, Tokyo, Japan). ECG-gated non-contrast chest CT was performed in advance, gated at 75% of the R-R interval, with a tube current of 50–250 mA, and a voltage of 120 kVp. CCTA was obtained in a single-heartbeat scan with a phase window of 70%–99% of the R-R interval, with a tube current of 50–900 mA, and a voltage of 100 kVp. Patients with a pre-scan heart rate ≥60 beats per minutes (bpm) were given 20–40 mg of metoprolol orally. If the heart rate remained ≥61 bpm after 1 h, they were given intravenous landiolol (0.125 mg/kg) (Corebeta: Ono Pharmaceutical, Tokyo, Japan). All patients received 0.6 mg nitroglycerin sublingually (Nitropen: Nipponkayaku, Tokyo, Japan). Patients were excluded with poor image quality (n = 6) and those lost to follow-up after less than 90 days (n = 23). Finally, 333 patients in total were enrolled in cohort 2. NC-PCAT and CACS were measured on ECG-gated non-contrast CT. The follow-up period began on the day of the CT scan and continued until the clinical endpoint or until the end of the study period (31 December 2020). Patients were observed for a median period of 2.9 years, and the primary endpoint was the composite of all-cause death and non-fatal MI. Demographic data and clinical information were collected retrospectively from the patients' medical records at our institution or by telephone interview. This retrospective study was approved by our institutional review board in accordance with local ethics procedures, and the requirement to obtain informed consent was waived.

2.2. Data measurement and analysis

2.2.1. Measurement of CACS

In both cohorts, CACS was measured using semi-automated dedicated software (Ziostation2, Ziosoft, Inc., Tokyo, Japan). As previously described in the literature [19], to detect CAC, a threshold of >130 Hounsfield Units (HU) was determined on an area of ≥ 1 mm^2, which corresponded to the default setting of the software.

2.3. Measurement of NC-PCAT

In both cohorts, the NC-PCAT value was obtained by measuring the mean CT value of pericardial fat on ECG-gated non-contrast CT. On an axial image, a 15 × 15 mm square region of interest (ROI) was placed on pericardial fat tissue dorsal and adjacent to the right coronary artery ostium (Fig. 2), and the mean CT value of all 225 pixels was calculated using an attenuation histogram. Using the method described previously

Table 1
Patient demographics and clinical characteristics according to cohort.

Variables	Cohort 1 (n = 300)	Cohort 2 (n = 333)
Age (years)	65.6 ± 11.9	68.3 ± 9.5
Male, n	172 (57.3%)	251 (75.4%)
Body mass index (kg/m^2)	23.6 ± 3.3	24.1 ± 3.4
Hypertension, n	169 (56.3%)	205 (61.6%)
Hyperlipidemia, n	145 (48.5%)	239 (71.8%)
Diabetes mellitus, n	98 (32.7%)	147 (44.1%)
Current smoking, n	41 (20.8%)	47 (14.1%)
Old cerebral infarction, n	12 (4.1%)	14 (4.2%)
CACS	18.18 [0, 189.9]	351.0 [130.7, 839.6]
CACS = 0, n	107 (35.7%)	10 (3.0%)
Ejection fraction (%)	63.9 ± 9.5	66.5 ± 8.0
PCAT (HU)	−81.3 ± 8.7	N/A
NC-PCAT (HU)	−90.8 ± 11.3	−93.0 ± 9.0
High risk plaque, n	34 (11.3%)	N/A

CACS = coronary artery calcium score; HU = Hounsfield unit; NC-PCAT = non-contrast pericoronary adipose tissue.

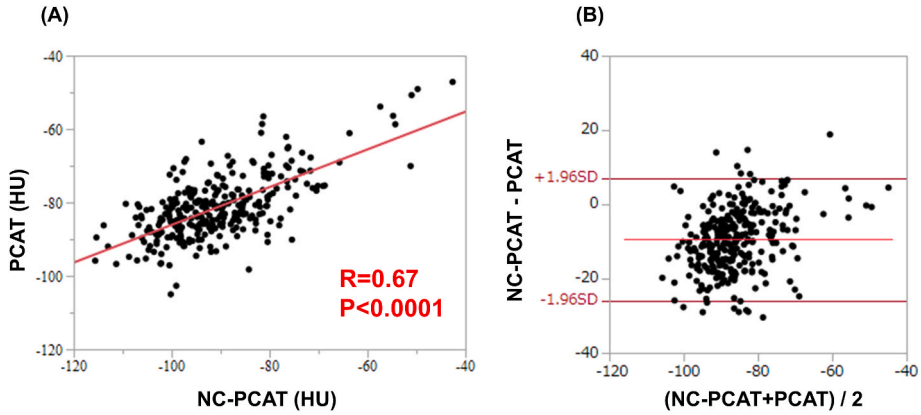

Fig. 3. (A) Simple linear regression model for PCAT and NC-PCAT. There is a good positive correlation between PCAT and NC-PCAT (R = 0.67, $p < 0.0001$). (B) Bland-Altman plots of PCAT and NC-PCAT. The mean difference is 9.4 HU, and only a few samples are located outside of 95% limits of agreement [-24.0, 7.2].

[20,21], CT values between −190 and −30 HU were considered to be pericoronary adipose tissue and values outside this range, which were considered to indicate other tissues such as vessel, myocardium, or calcification, were excluded. To ensure inter-observer reproducibility, the NC-PCAT values were assessed by two readers (A cardiologist with 8 years and a radiologist with 10 years of experience in cardiovascular imaging), and both were completely blinded to the each other's results.

2.4. Measurement of PCAT

In cohort 1, PCAT was measured by the conventional technique [10] on CCTA, using dedicated software (Aquarius iNtuition, Terarecon Inc., Foster City, CA, USA). On a tracing of the proximal 10–50 mm segment of the RCA, fat surrounding the outer vessel wall within 5 mm was regarded as PCAT. The PCAT value was defined as the mean CT value according to the attenuation histogram in the range of −190 to −30 HU,

Table 2
Logistic regression analysis for predicting high-risk plaque.

(A) Overall (n = 300)				
	Univariable OR (95%CI)	*p* value	Multivariable OR (95%CI)	*p* value
PCAT	1.07 (1.03–1.11)	0.0011		
NC-PCAT	1.05 (1.02–1.08)	0.0005	1.06 (1.03–1.10)	0.0001
Male	3.22 (1.35–7.65)	0.0041	2.25 (0.84–6.03)	0.11
Age	1.00 (0.97–1.03)	0.97		
Body mass index	1.03 (0.92–1.14)	0.64		
Hypertension	1.48 (0.71–3.12)	0.30		
Hyperlipidemia	1.60 (0.78–3.30)	0.20		
Diabetes mellitus	1.74 (0.84–3.59)	0.14		
Family history of CAD	1.31 (0.56–3.08)	0.55		
Current smoking	3.16 (1.38–7.22)	0.01	2.58 (1.03–6.49)	0.044
Old cerebral infarction	1.58 (0.33–7.51)	0.59		
Hemoglobin A1c	1.23 (0.96–1.58)	0.13		
HDL-Cholesterol	0.98 (0.96–1.00)	0.036	0.98 (0.96–1.00)	0.11
LDL-Cholesterol	1.00 (0.99–1.01)	0.76		
Triglyceride	1.00 (1.00–1.00)	0.96		
Serum creatinine	1.17 (0.65–2.10)	0.64		
CACS/10	1.01 (1.01–1.02)	0.0029	1.01 (1.00–1.02)	0.013
(B) CACS >0 (Nn= 193)				
	Univariable OR (95%CI)	*p* value	Multivariable OR (95%CI)	*p* value
PCAT	1.06 (1.02–1.11)	0.0026		
NC-PCAT	1.06 (1.02–1.09)	0.0005	1.06 (1.03–1.10)	0.002
Male	2.53 (1.04–6.16)	0.030	2.81 (1.06–7.48)	0.028
Age	0.97 (0.94–1.01)	0.11		
Body mass index	1.00 (0.89–1.12)	0.95		
Hypertension	1.03 (0.47–2.22)	0.95		
Hyperlipidemia	1.14 (0.53–2.41)	0.74		
Diabetes mellitus	1.54 (0.72–3.26)	0.27		
Family history of CAD	1.07 (0.89–2.58)	0.89		
Current smoking	3.26 (1.35–7.97)	0.012	3.02 (1.17–7.82)	0.027
Old cerebral infarction	1.34 (0.27–6.75)	0.73		
Hemoglobin A1c	1.20 (0.92–1.57)	0.19		
HDL-Cholesterol	0.99 (0.96–1.01)	0.19		
LDL-Cholesterol	1.00 (0.99–1.01)	0.77		
Triglyceride	1.00 (1.00–1.00)	0.93		
Serum creatinine	1.01 (0.52–1.97)	0.97		
CACS/10	1.01 (1.00–1.02)	0.15		

CACS = coronary artery calcium score; CAD = coronary artery disease; CI = confidence interval; HDL = high density lipoprotein; LDL-C = low density lipoprotein; NC-PCAT = non-contrast pericoronary adipose tissue; OR = odds ratio.

as described previously [10,22].

2.4.1. Definition of high-risk plaque identified on CCTA

The presence of HRP was assessed on CCTA. HRP was defined as coronary artery plaque with two or more of the following features: positive remodeling, low attenuation, spotty calcification, or napkin-ring sign on CCTA [23,24]. Positive remodeling was defined as the outer vessel diameter at the site of plaque divided by the average outer diameter of the proximal and distal vessels greater than 1.1. Low attenuation was defined as a non-calcified plaque with internal attenuation <30 HU. Spotty calcification was defined as punctate calcifications <3 mm diameter in any direction within the plaque, and napkin-ring sign was defined as a central low attenuation plaque surrounded by a region of higher CT attenuation.

2.4.2. Clinical endpoints

The primary endpoint was major adverse cardiac events (MACE), as the composite of all-cause death and non-fatal myocardial infarction (MI) up to a maximum of 5.8 years of follow-up. The composite of cardiac death and non-fatal MI was analyzed as the secondary outcome. Mortality data were obtained from the medical records of patients who died or who were treated at our institution, as well as from other hospitals to which patients had been admitted. Early revascularization is defined as that planned after the initial decision from within 90 days of CCTA. MI was defined as evidence of myocardial necrosis consistent with myocardial ischemia that occurred in a clinical setting [25].

2.4.3. Statistical analysis

In cohort 1, we compared NC-PCAT with PCAT graphically using Bland-Altman plots, and correlation metrics using linear regression analysis. Multivariable logistic regression analysis was used to evaluate the association between HRP and NC-PCAT and all other clinical characteristics, adjusting for factors that were significantly associated with the presence of HRP in univariable logistic regression analysis. In cohort 2, they were dichotomized (high/low NC-PCAT group) according to their median NC-PCAT (−93.55 HU). Survival curves were estimated using the Kaplan–Meier method and the log-rank test was used to detect statistically significant differences. Effects of the NC-PCAT on clinical outcomes were determined using multivariate Cox regression models, adjusted by age, sex, and early revascularization. Model diagnostics were used to evaluate proportional assumption. Normally distributed quantitative variables are presented as the mean and 95% confidence interval (CI). Non-normally distributed data are presented as the median and interquartile range (IQR). All statistical analyses were performed using JMP 14.2 (SAS Institute Inc., Cary, NC). Statistically significant difference was defined as a two-sided p value < 0.05.

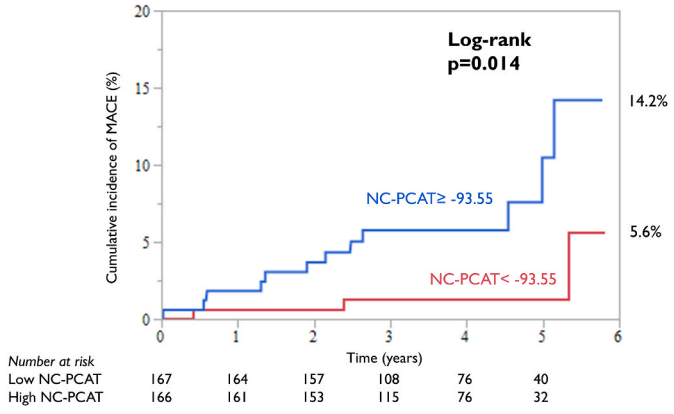

Fig. 4. Kaplan–Meier curves for the primary endpoint.
The cumulative incidence of MACE is significantly higher in the high NC-PCAT group compared to the low NC-PCAT group (log-rank $p = 0.014$).

Table 3
Cox hazard regression analysis for the primary endpoint.

	Univariable Hazard ratio (95%CI)	p value	Multivariable Hazard ratio (95%CI)	p value
NC-PCAT ≥ 93.55	4.30 (1.21–15.3)	0.011	4.28 (1.20–15.2)	0.012
Male	0.68 (0.23–2.00)	0.48	0.77 (0.25–2.36)	0.65
Age	1.03 (0.97–1.09)	0.34	1.02 (0.967–1.09)	0.45
Hypertension	1.32 (0.45–3.86)	0.61		
Hyperlipidemia	0.50 (0.18–1.41)	0.21		
Diabetes mellitus	0.84 (0.30–2.36)	0.74		
Current smoking	0.41 (0.05–3.12)	0.33		
CKD	0.67 (0.15–2.99)	0.59		
CACS ≥ 400	0.76 (0.27–2.14)	0.6		
Early revascularization	0.91 (0.32–2.56)	0.86	1.01 (0.35–2.87)	0.99

CACS = coronary artery calcium score; CI = confidence interval; CKD = chronic kidney disease; NC-PCAT = non-contrast pericoronary adipose tissue.

3. Results

3.1. Baseline and procedural characteristics

The demographic and clinical characteristics of each cohort are listed in Table 1. In cohort 1, 107/300 (35.7%) patients had no coronary calcification (CACS = 0), the mean NC-PCAT value was −90.8 HU, and the mean conventional PCAT value was −81.3 HU. In cohort 2, the mean NC-PCAT value was −93.0 HU.

3.2. Validity of NC-PCAT

There was a moderate positive correlation between PCAT and NC-PCAT (R = 0.67, $p < 0.0001$) (Fig. 3(A)). Bland-Altman plots are shown in Fig. 3(B), suggesting mean difference of 9.4 HU, and only a few samples are located outside the 95% limits of agreement [−26.0, 7.2]. There was good interobserver agreement for NC-PCAT (intraclass correlation coefficient: 0.807; 95%CI: 0.726–0.887; $p < 0.0001$).

3.3. Logistic regression analysis for HRP

Overall, HRP was found in 34/300 (11.3%) patients. Univariable logistic regression analysis identified PCAT, NC-PCAT, male sex, current smoking, high-density lipoprotein (HDL)-cholesterol, and CACS as significant indicators of HRP (Table 2(A)). Multivariable logistic regression analysis, NC-PCAT (odds ratio [OR] 1.06, 95%CI 1.03–1.10, $p = 0.0001$), CACS (OR 1.01 per 10 CACS increase, 95%CI 1.00–1.02, $p = 0.013$), and current smoking (OR 2.58, 95%CI 1.03–6.49, $p = 0.044$) were independent predictors of the presence of HRP. Among patients with CACS >0 (n = 193), PCAT, NC-PCAT, male sex, and current smoking were significantly associated with HRP in univariable logistic model, whereas CACS was not ($p = 0.15$) (Table 2(B)). When adjusted for these factors, NC-PCAT (OR 1.06, 95%CI 1.03–1.10, $p = 0.0002$), current smoking (OR 3.02, 95%CI 1.17–7.82, $p = 0.027$), and male sex (OR 2.81, 95%CI 1.06–7.48, $p = 0.028$) remained as independent predictors of the presence of HRP.

3.4. Clinical outcomes

The median duration of follow-up was 2.9 years (IQR 1.9–3.9) and MACE occurred in 16 (4.8%) patients during follow-up. There were 13 (3.9%) all-cause deaths and 3 (0.9%) cases of non-fatal MI. 138 patients (41.4%) underwent early revascularization. Fig. 4 shows Kaplan–Meier survival curves for the primary endpoint among patients, stratified by median NC-PCAT (−93.55 HU). The cumulative incidence of MACE was significantly higher in the high NC-PCAT group compared with the low NC-PCAT group (log-rank $p = 0.014$). The results of Cox proportional hazard regression analysis for the primary endpoint are shown in

Table 3. Univariable Cox hazard analysis revealed that only high NC-PCAT was significantly associated with high risk of MACE (hazard ratio [HR]: 4.3; 95%CI: 1.2–15.3; $p = 0.011$). When adjusted for age, sex, and early revascularization, high NC-PCAT remained an independent predictor of MACE (HR: 4.3; 95%CI: 1.2–15.2; $p = 0.012$). The results for the secondary endpoint are shown in the supplemental file. Similarly, Kaplan-Meier curves for the secondary endpoint suggest that the cumulative incidence of MACE is significantly higher in the high NC-PCAT group compared to the low NC-PCAT group (Supplemental Fig. 1, log-rank $p = 0.0068$). Multivariable Cox hazard analysis also revealed that high NC-PCAT was an independent predictor of MACE (HR: 10.1; 95%CI: 1.3–79.9; $p = 0.028$) (Supplemental Table 1). Model diagnostics were shown in Supplemental Table 2, suggesting that proportional assumption is maintained in each variable.

4. Discussion

There were three major findings of the present study. First, there was a good positive correlation between the NC-PCAT and conventional PCAT values, suggesting the validity of measuring pericoronary adipose tissue from non-contrast CT. Second, high value of NC-PCAT was an independent predictor of the presence of HRP. Moreover, among patients with coronary calcification, high CACS was not a predictor of HRP, regardless of the value. Third, high value of NC-PCAT was significantly associated with worse clinical outcome, composite all-cause death, and non-fatal MI.

Oikonomou et al. reported that high fatty attenuation index in the proximal RCA is predictive of all-cause and cardiac mortality and can be used as a representative biomarker of global coronary inflammation [13]. However, the conventional method for evaluating pericoronary fat requires injection of contrast medium, which is generally contraindicated in patients with active bronchial asthma, contrast allergy, or renal deficiency. Measurement of CACS on ECG-gated non-contrast CT is now widely accepted as a less invasive method of CAD risk stratification compared with conventional CCTA. From these points of view, we hypothesized that the value of NC-PCAT adjacent to the RCA ostium would reflect overall coronary inflammation, and that the combination of CACS and NC-PCAT would enable accurate screening for CAD for all patients, without requiring contrast medium. Despite variations in anatomy, there is usually sufficient pericardial fat surrounding the RCA ostium to enable assessment on axial CT, whereas the amount surrounding the left coronary artery can be insufficient. For this reason, we set the ROI beside the RCA ostium. As shown in Table 1, the mean value of NC-PCAT was 9.4 HU lower than that of PCAT, which was probably due to partial volume effect, beam hardening, or other radiographic conditions. Partial volume effect is inevitable in quantifying CT values of pixels that are back-to-back with enhanced coronary artery lumen, and beam hardening artifact is caused by extracellular distribution of contrast media. Although we set threshold CT values for defining NC-PCAT between −190 and −30 HU, which have been commonly used in previous studies [26,27], there is no consensus regarding the threshold values for identifying pericoronary fat tissue.

Based on our finding that the value of NC-PCAT correlated well with that of PCAT, which is significantly associated with HRP [11,12], we hypothesized that NC-PCAT has potential to indicate the presence of HRP, which is itself associated with increased cardiovascular risk [28]. Previous studies have reported a relationship of HRP with coronary vascular inflammation [12], but not with coronary calcification [29]. However, the results of the present study revealed both NC-PCAT and CACS as independent predictors of HRP, presumably because cohort 1 included many 'calcium-absent' low risk patients (35.7%) who did not have HRP as a matter of course. However, our subgroup analysis revealed that in patients with CACS >0, CACS lost its predictive value for HRP, whereas NC-PCAT retained its significance. In other words, only NC-PCAT could predict the presence of HRP in intermediate to high-risk patients. According to these facts, we focused on intermediate to high-risk patients for prognostic analysis and enrolled only patients with 50%–90% coronary luminal stenosis to cohort 2.

The ultimate finding of this study was that high NC-PCAT values, but not CACS values, could predict worse clinical outcome. Cohort 2 comprised only CAD patients with a 50%–90% stenotic lesion, including those who underwent early revascularization. This means that CACS was not useful for risk stratification among patients with moderate to severe coronary stenosis or patients after revascularization of luminal coronary stenosis, and that NC-PCAT appears to be an alternative biomarker for anticipating future events in this patient group, possibly because NC-PCAT indicates coronary inflammation leading to ACS, rather than obstructive CAD. Moreover, among all-cause deaths in cohort 2, 5/13 patients died of cancer, which might suggest the contribution of systemic inflammation driven by cancer to elevation of NC-PCAT values. Indeed, previous studies have demonstrated that exposure to chronic systemic inflammation is related to coronary atherogenesis [30] and that some anti-inflammatory agents can lower the incidence of cardiovascular events [31–33]. In the present study, however, NC-PCAT also showed a significant association with cardiac death and MI (secondary endpoint); therefore, further evaluation is needed to clarify whether or not NC-PCAT indicates systemic inflammation. The present results suggest that combined assessment using CACS in low-risk patients and NC-PCAT in intermediate (or high) risk patients might be effective for predicting worse clinical outcome in the whole population.

Our study has some limitations. First, it was a single-center retrospective study in Japan with a relatively small cohort, and all imaging was obtained using the same CT scanner. It is necessary to confirm our results in a larger multiracial participant group under different scan conditions. Second, the method for quantification of NC-PCAT remains controversial. In our experience, 15 mm square ROI is the largest frame that can be placed at the area adjacent to the RCA, however, as compared to the conventional PCAT quantification, this relatively small and uniplanar ROI might be lacking in generality. The NC-PCAT values calculated by the present method might vary depending on patient's anatomy. For example, we had difficulty setting the ROI on the fixed area in several patients whose RCA skirted the Valsalva sinus. Accordingly, it was necessary to place the ROI on an image several slices higher or lower, or on the ventral side of the RCA. Nonetheless, there was good correlation between NC-PCAT and PCAT, and both were significant indicators of HRP in univariable logistic regression analysis. Third, as described above, the threshold for identifying NC-PCAT remains unclear. It is also necessary to confirm the present results using other threshold settings in the future. Fourth, we investigated clinical outcomes by retrospectively referring medical records and telephone interview to all the participants, however, some MACEs could not be identified and it might affect the net result. We should also state that no information about medication was considered, which might affect the plaque quality and quantity. Finally, regarding cohort 2, conventional PCAT was not measured to investigate prognosis, because in this present study, we found a value in evaluating it without use of contrast. If compared a prognostic impact between two methods, it would be more interesting. And since the number of sequential patients with ACS was very small (n = 3), the prognostic value of NC-PCAT for future ACS should be revalidated in a larger cohort.

In conclusion, NC-PCAT values correlated well with those of conventional PCAT and were significantly associated with the presence of HRP. High NC-PCAT value was a significant predictor of worse clinical outcome in CAD patients with moderate to severe stenosis.

CRediT authorship contribution statement

Daigo Takahashi: Validation, Data curation, Formal analysis, Investigation, Writing – original draft. **Shinichiro Fujimoto:** Conceptualization, Methodology, Supervision. **Yui O. Nozaki:** Formal analysis, Data curation. **Ayako Kudo:** Formal analysis, Data curation. **Yuko O. Kawaguchi:** Formal analysis, Data curation. **Kazuhisa Takamura:**

Formal analysis, Data curation. **Makoto Hiki:** Formal analysis, Data curation. **Hideyuki Sato:** Formal analysis. **Nobuo Tomizawa:** Formal analysis. **Kanako K. Kumamaru:** Writing – review & editing. **Shigeki Aoki:** Writing – review & editing, Supervision. **Tohru Minamino:** Writing – review & editing, Supervision.

Declaration of competing interest

The authors declare that they have no known competing financial interests or personal relationships that could have appeared to influence the work reported in this paper.

Acknowledgements

The authors are grateful to Yosuke Kogure, RT, Hidekazu Inage, RT, and Hideyuki Sato, RT, for technical assistance in this study.

Appendix A. Supplementary data

Supplementary data to this article can be found online at https://doi.org/10.1016/j.atherosclerosis.2023.01.021.

References

[1] R. Ross, Atherosclerosis — an inflammatory disease, N. Engl. J. Med. 340 (2) (1999) 115–126.
[2] M. Konishi, S. Sugiyama, Y. Sato, S. Oshima, K. Sugamura, T. Nozaki, et al., Pericardial fat inflammation correlates with coronary artery disease, Atherosclerosis 213 (2) (2010) 649–655.
[3] M.C. Fishbein, R.J. Siegel, How big are coronary atherosclerotic plaques that rupture? Circulation 94 (10) (1996) 2662–2666.
[4] M.R. Dweck, Z.A. Fayad, Imaging: perivascular fat - an unheralded informant of coronary inflammation, Nat. Rev. Cardiol. 14 (10) (2017) 573–574.
[5] R. Nakazato, H. Otake, A. Konishi, M. Iwasaki, B.K. Koo, H. Fukuya, et al., Atherosclerotic plaque characterization by CT angiography for identification of high-risk coronary artery lesions: a comparison to optical coherence tomography, Eur. Heart J. Cardiovasc. Imag. 16 (4) (2015) 373–379.
[6] G. Feuchtner, J. Kerber, P. Burghard, W. Dichtl, G. Friedrich, N. Bonaros, et al., The high-risk criteria low-attenuation plaque <60 HU and the napkin-ring sign are the most powerful predictors of MACE: a long-term follow-up study, Eur. Heart J. Cardiovasc. Imag. 18 (7) (2017) 772–779.
[7] M. Ferencik, T. Mayrhofer, D.O. Bittner, H. Emami, S.B. Puchner, M.T. Lu, et al., Use of high-risk coronary atherosclerotic plaque detection for risk stratification of patients with stable chest pain: a secondary analysis of the PROMISE randomized clinical trial, JAMA Cardiol. 3 (2) (2018) 144–152.
[8] P. Maurovich-Horvat, C.L. Schlett, H. Alkadhi, M. Nakano, F. Otsuka, P. Stolzmann, et al., The napkin-ring sign indicates advanced atherosclerotic lesions in coronary CT angiography, JACC Cardiovasc. Imag. 5 (12) (2012) 1243–1252.
[9] F. Prati, V. Marco, G. Paoletti, M. Albertucci, Coronary inflammation: why searching, how to identify and treat it, Eur. Heart J. Suppl. 22 (Supplement_E) (2020) E121–E124.
[10] A.S. Antonopoulos, F. Sanna, N. Sabharwal, S. Thomas, E.K. Oikonomou, L. Herdman, et al., Detecting human coronary inflammation by imaging perivascular fat, Sci. Transl. Med. 9 (398) (2017), eaal2658.
[11] X. Chen, Y. Dang, H. Hu, S. Ma, Y. Ma, K. Wang, et al., Pericoronary adipose tissue attenuation assessed by dual-layer spectral detector computed tomography is a sensitive imaging marker of high-risk plaques, Quant. Imag. Med. Surg. 11 (5) (2021) 2093–2103.
[12] J. Yuvaraj, A. Lin, N. Nerlekar, R.K. Munnur, J.D. Cameron, D. Dey, et al., Pericoronary adipose tissue attenuation is associated with high-risk plaque and subsequent acute coronary syndrome in patients with stable coronary artery disease, Cells 10 (5) (2021).
[13] E.K. Oikonomou, M. Marwan, M.Y. Desai, J. Mancio, A. Alashi, E. Hutt Centeno, et al., Non-invasive detection of coronary inflammation using computed tomography and prediction of residual cardiovascular risk (the CRISP CT study): a post-hoc analysis of prospective outcome data, Lancet 392 (10151) (2018) 929–939.
[14] J. Knuuti, W. Wijns, A. Saraste, D. Capodanno, E. Barbato, C. Funck-Brentano, et al., ESC Guidelines for the diagnosis and management of chronic coronary syndromes, Eur. Heart J. 41 (3) (2019) 407–477, 2020.
[15] M. Writing Committee, M. Gulati, P.D. Levy, D. Mukherjee, E. Amsterdam, D. L. Bhatt, et al., AHA/ACC/ASE/CHEST/SAEM/SCCT/SCMR guideline for the evaluation and diagnosis of chest pain: a report of the American College of Cardiology/American heart association joint committee on clinical practice guidelines, J. Am. Coll. Cardiol. 78 (22) (2021) e187–e285, 2021.
[16] T. Misaka, T. Furukawa, N. Asato, M. Uemura, R. Ashikaga, T. Ishida, Perivascular fat attenuation index on non-contrast-enhanced cardiac computed tomography: comparison with coronary computed tomography angiography, Open J. Radiol. 10 (2020) 138–148, 03.
[17] S. Almeida, M. Pelter, K. Shaikh, L. Cherukuri, D. Birudaraju, K. Kim, et al., Feasibility of measuring pericoronary fat from precontrast scans: effect of iodinated contrast on pericoronary fat attenuation, J. Cardiovasc. Comput. Tomogr. 14 (6) (2020) 490–494.
[18] X.Y. Jiang, Z.Q. Shao, Y.T. Chai, Y.N. Liu, Y. Li, Non-contrast CT-based radiomic signature of pericoronary adipose tissue for screening non-calcified plaque, Phys. Med. Biol. 67 (10) (2022).
[19] A.S. Agatston, W.R. Janowitz, F.J. Hildner, N.R. Zusmer, M. Viamonte, R. Detrano, Quantification of coronary artery calcium using ultrafast computed tomography, J. Am. Coll. Cardiol. 15 (4) (1990) 827–832.
[20] M. Sadouni, I. Boldeanu, M. Durand, D. Juneau, S. Blais, C. Tremblay, et al., Quantification of epicardial fat using non contrast cardiac CT in an HIV population: reproducibility and association with other body fat indices, Eur. J. Radiol. Open 8 (2021), 100317.
[21] F. Commandeur, M. Goeller, J. Betancur, S. Cadet, M. Doris, X. Chen, et al., Deep learning for quantification of epicardial and thoracic adipose tissue from non-contrast CT, IEEE Trans. Med. Imag. 37 (8) (2018) 1835–1846.
[22] M. Goeller, B.K. Tamarappoo, A.C. Kwan, S. Cadet, F. Commandeur, A. Razipour, et al., Relationship between changes in pericoronary adipose tissue attenuation and coronary plaque burden quantified from coronary computed tomography angiography, Eur. Heart J. Cardiovasc. Imag. 20 (6) (2019) 636–643.
[23] R.C. Cury, S. Abbara, S. Achenbach, A. Agatston, D.S. Berman, M.J. Budoff, et al., CAD-RADS(TM) coronary artery disease - reporting and data system. An expert consensus document of the society of cardiovascular computed tomography (SCCT), the American College of Radiology (ACR) and the North American Society for cardiovascular imaging (NASCI). Endorsed by the American College of Cardiology, J. Cardiovasc. Comput. Tomogr. 10 (4) (2016) 269–281.
[24] L.J. Shaw, R. Blankstein, J.J. Bax, M. Ferencik, M.S. Bittencourt, J.K. Min, et al., Society of cardiovascular computed tomography/North American Society of cardiovascular imaging - expert consensus document on coronary CT imaging of atherosclerotic plaque, J. Cardiovasc. Comput. Tomogr. 15 (2) (2021) 93–109.
[25] K. Thygesen, J.S. Alpert, A.S. Jaffe, B.R. Chaitman, J.J. Bax, D.A. Morrow, et al., Fourth Universal Definition of myocardial infarction (2018), Circulation 138 (20) (2018) e618–e651.
[26] J. Ding, F.C. Hsu, T.B. Harris, Y. Liu, S.B. Kritchevsky, M. Szklo, et al., The association of pericardial fat with incident coronary heart disease: the Multi-Ethnic Study of Atherosclerosis (MESA), Am. J. Clin. Nutr. 90 (3) (2009) 499–504.
[27] M. Marwan, S. Koenig, K. Schreiber, F. Ammon, M. Goeller, D. Bittner, et al., Quantification of epicardial adipose tissue by cardiac CT: influence of acquisition parameters and contrast enhancement, Eur. J. Radiol. 121 (2019), 108732.
[28] E. Conte, A. Annoni, G. Pontone, S. Mushtaq, M. Guglielmo, A. Baggiano, et al., Evaluation of coronary plaque characteristics with coronary computed tomography angiography in patients with non-obstructive coronary artery disease: a long-term follow-up study, Eur. Heart J. Cardiovasc. Imag. 18 (10) (2017) 1170–1178.
[29] L.J. Heinsen, G. Pararajasingam, T.R. Andersen, S. Auscher, H.M. Sheta, H. Precht, et al., High-risk coronary artery plaque in asymptomatic patients with type 2 diabetes: clinical risk factors and coronary artery calcium score, Cardiovasc. Diabetol. 20 (1) (2021) 164.
[30] C.E. Kosmas, D. Silverio, A. Sourlas, P.D. Montan, E. Guzman, M.J. Garcia, Anti-inflammatory therapy for cardiovascular disease, Ann. Transl. Med. 7 (7) (2019) 147.
[31] P.M. Ridker, B.M. Everett, T. Thuren, J.G. MacFadyen, W.H. Chang, C. Ballantyne, et al., Antiinflammatory therapy with Canakinumab for atherosclerotic disease, N. Engl. J. Med. 377 (12) (2017) 1119–1131.
[32] K. Vaidya, C. Arnott, G.J. Martinez, B. Ng, S. McCormack, D.R. Sullivan, et al., Colchicine therapy and plaque stabilization in patients with acute coronary syndrome: a CT coronary angiography study, JACC Cardiovasc. Imag. 11 (2 Pt 2) (2018) 305–316.
[33] S.M. Nidorf, J.W. Eikelboom, C.A. Budgeon, P.L. Thompson, Low-dose colchicine for secondary prevention of cardiovascular disease, J. Am. Coll. Cardiol. 61 (4) (2013) 404–410.